Macromolecules
ARTICLE

Macromolecules **2010**, *43*, 1245–1252 **1245**
DOI: 10.1021/ma9026614

Synthesis and Assembly Behavior of Heteronucleobase-Functionalized Poly(ε-caprolactone)

I-Hong Lin, Chih-Chia Cheng, Ying-Chieh Yen, and Feng-Chih Chang*

Institute of Applied Chemistry, National Chiao Tung University, HsinChu, Taiwan

Received December 1, 2009; Revised Manuscript Received January 6, 2010

ABSTRACT: The heteronucleobase (adenine and uracil)-functionalized poly(ε-caprolactone) (A-PCL-U) possessing supramolecular structure has been successfully synthesized through the combination of ring-opening polymerization and Michael addition reaction. Attachment of multiple hydrogen-bonding units to chain ends of PCL results in phase separation and substantial increase in the viscosity. The association constant (K_a) between adenine and uracil groups of A-PCL-U calculated from NMR measurement is 18.9 M^{-1}. XRD and DSC analyses indicate that the crystalline structure of the A-PCL-U is changed to some extent due to phase segregation as compared to the PCL homopolymer. The AFM micrograph demonstrates that phase segregation is formed from the hard nucleobase chain ends and the soft poly(ε-caprolactone) chains of the supramolecular complex.

Introduction

In both DNA and RNA, hydrogen-bonding interaction has drawn a great deal of interest because of novel structure organizations.[1−3] Biomimetic polymers with moderately strong and highly directional molecular recognitions exhibit unique physical properties, such as high specificity, controlled affinity, and reversibility.[4−16] Biocompatible and biodegradable polymers containing multiple hydrogen bondings have received significant interest in applications such as surgical fixation devices, controlled drug delivery, and tissue engineering scaffolds.[17,18] However, reports on synthetic biocompatible and biodegradable polymers containing nucleobase molecular recognition sites are still rare.[19−22] It is still a challenge to control the supramolecular polymers with secondary (and higher) bonding through specific interactions from different hydrogen-bonding motifs.[23]

In order to utilize the complementary nature of nucleobase pairs, numerous reports regarding the effect of the placement of chain ends on polymers or small molecules using supramolecular motifs on material properties have been reported.[24−27] Meijer et al.[28] recently reported the synthesis of oligomeric poly(ε-caprolactone)s containing self-complementary quadruple-hydrogen-bonding 2-ureido-4[1*H*]-pyrimidinone (UPy) units. Mixing of the UPy-functionalized poly(ε-caprolactone) with UPy-functionalized peptides results in bioactive supramolecular structure that exhibits strong and specific cell binding properties. Sivakova et al.[29,30] developed low molecular weight poly(tetrahydrofuran) consisting of modified nucleobase moieties and possesses free-standing film behavior. Besides functionalizing chain ends of polymers, it is also possible to place nucleobases on polymer side chains.[31−33] For side-chain architectures, these proton donors and acceptors are appended to polymers that have main chains in forms of homo- or block copolymers and which the self-assembly occurs via hydrogen bonding interaction, usually in multiple fashion. For instance, Rotello and co-workers[34] have studied low molecular weight polystyrene derivatized with diamidopyridine units which can be noncovalently cross-linked with bis-thymine units. Such nucleobase end-functionalized strategies have become a critical component of polymer science and are expected to expand further in the future.

In biological systems, complementary multiple-hydrogen-bonding interactions are paramount and the basic concept of molecular recognition which occurs in adenine−thymine (A−T) and guanine−cytosine (G−C) base pairs in DNA.[35] A wide variety of synthetic polymers were functionalized with the self-complementary nucleobases, such as adenine, thymine, and uracil;[15,26,29,36] however, reports describing the incorporation of heteronucleobase unit in biocompatible materials are rare.[37−39] We have studied the biocomplementary interactions of a DNA-like side-chain homopolymer with alkylated nucleobases mediated by hydrogen-bonded thymine−adenine (T−A) base pairs.[40] Recently, we also reported that the interassociation equilibrium constant (K_a) between adenine (A) and uracil (U) is of ca. 671 M^{-1}, which is stronger than that between adenine (A) and thymine (T) (ca. 534 M^{-1}).[41] Taking the above discussion into account, poly(ε-caprolactone) with molecular recognition units of adenine−uracil (A−U) base pairs was prepared, and the bioactivity was introduced into poly(ε-caprolactone) through the combination of ring-opening-polymerization and quantitative Michael addition strategies. The supramolecular polymerization and self-assembly behaviors of the new poly(ε-caprolactone) derivative through complementary A−U pairs were analyzed using ^{1}H NMR titration, wide-angle X-ray diffraction (WAXD), Fourier transform infrared (FTIR), differential scanning calorimetry (DSC), Ubbelohde viscometer, and atomic force microscopy (AFM).

Experimental Section

Materials. ε-Caprolactone (ε-CL, 99.5%, ACROS), dimethyl sulfoxide (DMSO, 99%, ACROS), and dimethylformamide (DMF, 99%, Fisher Chemical) were dried over calcium hydride (CaH_2, 95%, ACROS) for 24 h and then distilled under reduced pressure prior to use. Uracil (U, 99%, ACROS), adenine (A, 99%, Sigma), triethylaluminum ($AlEt_3$, 0.9 M in hexane, Fluka), glacial acetic acid (HPLC grade, TEDIA), ethylene carbonate (99%, Aldrich), sodium hydroxide (NaOH, 99%, Acros), acryloyl chloride (97%, Alfa Aesar), tetrahydrofuran

*Corresponding author. E-mail: changfc@mail.nctu.edu.tw.

Published on Web 01/14/2010

Scheme 1. Synthetic Route to Nucleobase-Terminated PCL

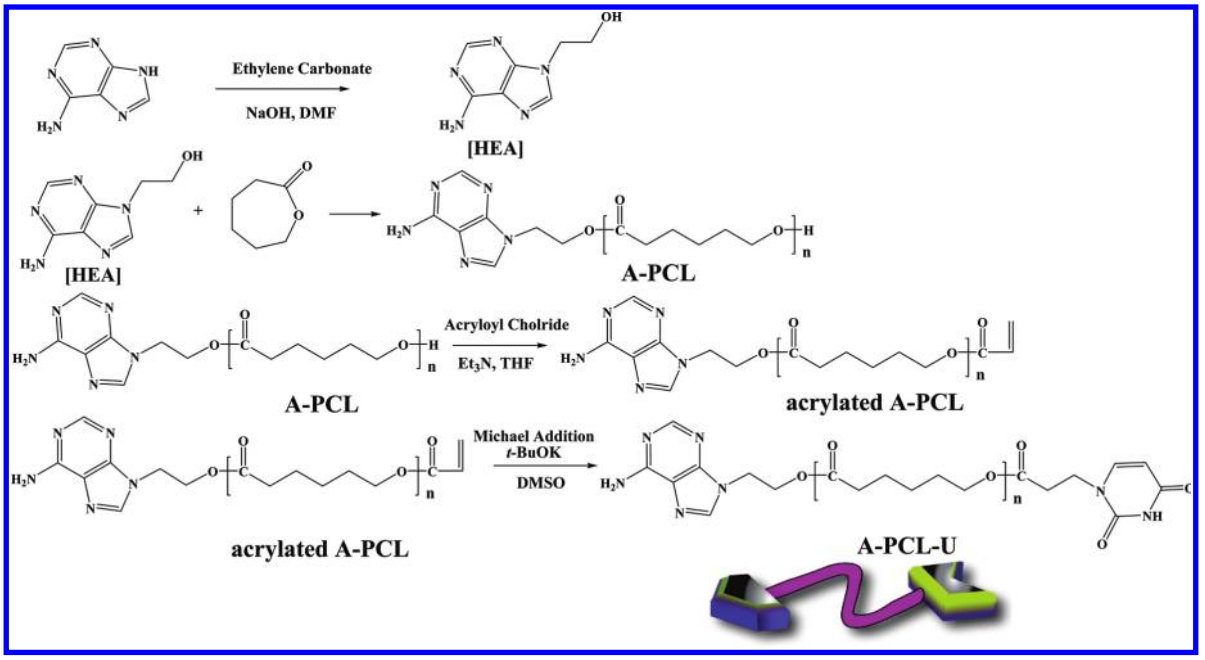

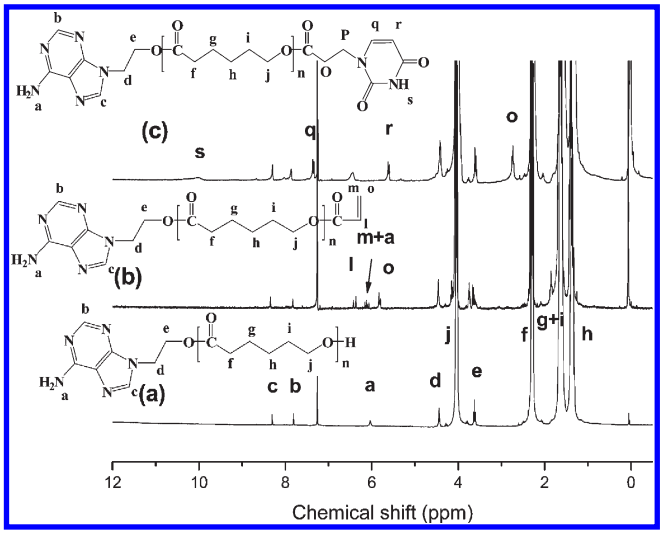

Figure 1. Stacked ^{1}H NMR spectra of (a) hydroxyl-terminated A-PCL, (b) acrylated-terminated A-PCL, and (c) uracil nucleobase-terminated A-PCL-U (M_n = 4023 g/mol, M_w/M_n = 1.03).

(THF, HPLC grade, TEDIA), potassium *tert*-butoxide (*t*-BuOK, 97%, Fluka), and methanol (MeOH, HPLC grade, TEDIA) were all used as received. Control PCL was obtained by ring-opening polymerization as previously described, and it has a quoted molecular weight of M_n = 5524.[42]

Synthetic Routes. Adenine−uracil nucleobase-terminated PCL, A-PCL-U, was synthesized via a four-step synthesis as shown in Scheme 1. In the first step, adenine is condensed with ethylene carbonate in hot DMF to afford the intermediate 9-(2′-hydroxyethyl)adenine [HEA] with 70% yield after recrystallization from ethanol as reported earlier.[43] Through the second step, the ring-opening polymerization of ε-caprolactone (ε-CL) initiated by 9-(2-hydroxyethyl)adenine [HEA] using $Al(Et)_3$ as a catalyst produces PCL containing adenine-functionalized chain end with narrow molar mass distributions (M_w/M_n = 1.03−1.08). Then, acryloyl chloride was reacted with terminal hydroxyl groups of A-PCL in THF solution to introduce the acrylate end group. ^{1}H NMR spectroscopy further confirms quantitatively end-group functionalization (Figure 1) on the basis of the concurrent appearance of resonances l, m, and o at 6.38, 6.12, and 5.80 ppm, respectively, which are assigned to the olefinic protons of the acrylate-terminated PCL prepolymer. Finally, Micheal addition of the acrylated A-PCL with heterocyclic uracil results in adenine−uracil nucleobase-terminated PCL [A-PCL-U] with complementary multiple-hydrogen-bonding end groups.

Synthesis of 9-(2′-Hydroxyethyl)adenine [*HEA*]. A solution of adenine (4.96 g, 36.7 mmol), ethylene carbonate (3.30 g, 37.5 mmol), and a trace of NaOH in DMF (150 mL) was heated to reflux for 2 h. After filtration and removal of the solvent under reduced pressure, the crude product was recrystallized from ethanol to give 4.68 g (71%) of 9-(2′-hydroxyethyl)adenine [HEA] as colorless powder; mp 232−234 °C. Quantitative functionalization was confirmed using ^{1}H NMR spectroscopy. ^{1}H NMR (500 MHz, DMSO, δ): 8.14 (1 H, s, ArH), 8.08 (1 H, s, ArH), 7.18 (2 H, s, NH_2), 5.00 (1 H, t, J = 5.4 Hz, OH), 4.19 (2 H, t, J = 5.5 Hz, CH_2), 3.75 (2 H, q, J = 5.4 Hz, CH_2).

Preparation of the Prepolymer of Adenine-End-Capped PCL (*A-PCL*). 0.2 mL of a toluene solution of triethyaluminum (0.1 mol/L) was added into the DMSO (5 mL) solution containing 9-(2′-hydroxyethyl)adenine [HEA] (0.1375 g, 8.3 × 10^{-4} mol) under an argon atmosphere. The mixture was stirred at 27 °C for 30 min and then evaporated to dryness, and the byproduct 2-propanol was removed. After repeating this procedure three times, 5 mL of caprolactone (0.044 mol) dissolved in 25 mL of dry DMSO was added to the reaction mixture maintained at 0 °C. The mixture was maintained at 27 °C for 4 h under an argon atmosphere, and the reaction was terminated by adding excess acetic acid (0.2 mL of acetic acid/0.8 mL of DMSO). Two-thirds of the initial solvent was evaporated, and the residue was precipitated into methanol. The product was dried until constant weight under vacuum and gave yield of 3.6 g (74%). Quantitative functionalization was confirmed using ^{1}H NMR spectroscopy. ^{1}H NMR (500 MHz, $CDCl_3$, δ): 8.3 (1H, −N=C*H*N−), 7.8 (1H, =NC*H*=N−), 6.0 (2H, −NH_2), 3.9−4.2 (polycaprolactone, 2H per repeating unit, −COOCH_2−), 4.4 (2H, −NCH_2CH_2−), 3.6 (2H, −NCH_2CH_2−), 2.1−2.4 (polycaprolactone, 2H per repeating unit, −CO=CH_2CH_2−), 1.5−1.8 (polycaprolactone, 2H per repeating unit, −COCH_2CH_2−, 2H per repeating unit, −COOCH_2CH_2−), 1.2−1.4 (polycaprolactone, 2H per repeating unit, −COCH_2CH_2CH_2−).

Synthesis of Acrylated A-PCL. A-PCL (3.6 g, 6.8×10^{-4} mol) was added under nitrogen into a 100 mL flame-dried, septum-sealed, two-neck, round-bottomed flask with a magnetic stir bar. The flask was equipped with an addition funnel and placed in ice bath. Tetrahydrofuran (THF) (50 mL) was added under nitrogen to prepare an 8 wt % polymer solution. Triethylamine (TEA) (3-fold excess, 0.25 mL) in 5 mL of THF was added by syringe into the reaction mixture under nitrogen, and the mixture was cooled to 0 °C. Acryloyl chloride (3-fold excess, 0.2 mL) dissolved in 10 mL of THF and syringed into the addition funnel dropwisely to the reaction mixture under nitrogen. The reaction was performed for 24 h at 27 °C, and the mixture was filtered to remove triethylamine hydrochloride salt. The THF was removed using rotary evaporation, and the product was redissolved in chloroform, precipitated repeatedly into methanol, and dried under reduced pressure at 25 °C for 24 h, giving yield of 3.2 g (88%). Quantitative functionalization was confirmed using ^{1}H NMR spectroscopy. ^{1}H NMR (500 MHz, $CDCl_3$, δ): 5.8−6.5 (3H, $-OCCH{=}CH_2$,), 8.3 (1H, $-N{=}CHN-$), 7.8 (1H, $=NCH{=}N-$), 6.0 (2H, $-NH_2$), 3.9−4.2 (polycaprolactone, 2H per repeating unit, $-COOCH_2-$), 4.4 (2H, $-NCH_2CH_2-$), 3.6 (2H, $-NCH_2CH_2-$), 2.1−2.4 (polycaprolactone, 2H per repeating unit, $-CO{=}CH_2CH_2-$), 1.5−1.8 (polycaprolactone, 2H per repeating unit, $-COCH_2CH_2-$, 2H per repeating unit, $-COOCH_2CH_2-$), 1.2−1.4 (polycaprolactone, 2H per repeating unit, $-COCH_2CH_2CH_2-$).

Synthesis of Heteronucleobase-Functionalized A-PCL-U. The acrylated A-PCL (3.2 g) was added under nitrogen to a flame-dried, 50 mL round-bottomed flask containing a magnetic stir bar. Potassium *tert*-butoxide (10 mg) was added as a catalyst under nitrogen, and the flask was sealed with a rubber septum. 3.6 g (22-fold molar excess) of uracil was dissolved separately in 60 mL of DMSO maintained at 120 °C, and the solution was cooled to 60 °C after uracil was completely dissolved; then the solution was added by syringe into the A-PCL reaction mixture under nitrogen maintained at 60 °C. The reaction was allowed to proceed for 3 days, and during this time, the uracil was precipitated partially. The mixture was filtered, and the DMSO was removed at 60 °C and 100 mTorr. The product was redissolved in chloroform, precipitated into methanol, and dried under reduced pressure at 50 °C for 24 h, resulting product yield 2.5 g (78%). Quantitative functionalization was confirmed using ^{1}H NMR spectroscopy. ^{1}H NMR (500 MHz, $CDCl_3$, δ): 9.7−10.2 (1H, $-CONHCO-$), 7.2−7.5 (1H, $-NCH-$), 5.5−5.7 (1H, $-COCH-$), 2.6−2.8 (2H, $-OCOCH_2CH_2N-$). M_n was calculated from the relative ^{1}H NMR integration ratio of PCL methylene protons ($-OC{=}OCH_2-$) at 3.8−4.2 ppm compared to the primary amino protons of the adenine unit (2H, $-NH_2$) at 6.0 ppm.

Characterizations. FTIR spectra were recorded using a Nicolet Avatar 320 FTIR spectrometer; 32 scans were collected at a spectral resolution of 1 cm^{-1}. The conventional KBr disk method was employed: the sample was dissolved in THF, then cast onto a KBr disk, and dried under vacuum at 80 °C. ^{1}H NMR spectra were recorded on a Varian Inova 500 MHz spectrometer equipped with a 9.395 T Bruker magnet and operated at 500 MHz. The weight-average molecular weight (M_w), number-average molecular weight (M_n), and PDI (M_w/M_n) were measured using a Waters 410 GPC system equipped with a refractive index detector and three Ultrastyragel columns (100, 500, and 1000 Å) connected in series. The system was calibrated using polystyrene (PS) standards. Thermal analysis was carried out using a DSC instrument (TA Instruments Q-20) under an atmosphere of dry N_2. Samples were weighed (3−5 mg) and sealed in an aluminum pan, which was scanned from 30 to 160 °C at a scan rate of 20 °C/min. WAXD spectra of powders were obtained using a Rigaku D/max-2500 X-ray diffractometer. The radiation source was Ni-filtered Cu Kα radiation at a wavelength of 0.154 nm. The voltage and current were set at 30 kV and 20 MA, respectively. Bragg's law ($\lambda = 2d \sin\theta$) was used to compute the *d*-spacing corresponding to the complementary behavior. Real-time small-angle X-ray scattering (SAXS) measurement was performed at BL01B SWLS beamline in the National Synchrotron Radiation Research Center (NSRRC), Taiwan. The incident X-ray beam was focused vertically by a mirror and monochromated to the energy of 10.5 keV by a germanium (111) double-crystal monochromator. The wavelength (λ) of the X-ray beam was 1.180 95 Å. AFM micrographs were recorded at 37 °C in air using a Digital Instrument Multimode Nanoscope IV operating in the tapping regime mode using silicon cantilever tips (PPP-NCH-50, 204−497 kHz, 10−130 N/m).

Table 1. Results of Polymerization for Adenine−Uracil Nucleobase-Terminated PCL with Different Molecular Weights

entry	[M]/[I][a]	$M_{n,NMR}$[b]	$M_{n,theo}$[c]	M_w/M_n[d]
control PCL 5K	60/1	5524	5782	1.38
A-PCL-U 10K	100/1	9242	9970	1.07
A-PCL-U 5K	64/1	5113	5880	1.08
A-PCL-U 4K	45/1	4023	4430	1.03

[a] M = CL, I = initiator. [b] $M_{n,NMR}$ was determined on the basis of the integral ratio of the methylene signal on the PCL polymer backbone ($-OC{=}OCH_2-$, 3.9−4.2 ppm) and signal on the primary amine end group (NH_2-, 6.0 ppm). [c] $M_{n,theo}$ = ([M]/[I] × M_{CL} + M_I) × yield; $M_{n,theo}$ denotes the theoretical number-average molecular weight of PCL. [d] Weight-average molecular weight (M_w) and number-average molecular weight (M_n) are determined by GPC.

Results and Discussion

Characterizations of A-PCL-U Polymers. Successful incorporation of heterocyclic uracil motif is confirmed using ^{1}H NMR spectroscopy. The olefinic proton at 5.8−6.4 ppm disappears, confirming the completion of Micheal addition between the heterocyclic uracil unit and the acrylated A-PCL. Four new resonances characteristic of uracil are observed in the ^{1}H NMR spectrum of A-PCL-U at 10.2 ppm (s, $-CONHCO-$), 7.35 ppm (q, $-N-CH-$), 5.60 ppm (r, $-CONH-$), and 2.72 ppm (o, $-OCOCH_2CH_2N-$). Methylene resonances (p, $-OCOCH_2CH_2N-$) associated with ester are overlapped with the methylene protons in the PCL repeat units at 3.9−4.2 ppm. The formation of complementary multiple hydrogen bonding was characterized via the analysis of A-PCL-U as a 2.5 wt % (0.75 mM) solution in chloroform-*d*. The ^{1}H NMR resonances of the A-PCL-U are compared with the A-PCL precursor. Except for the NH protons (changed from 6.00 to 6.44 ppm), all these resonances of the A-PCL-U remain unshifted from their original chemical shifts in the corresponding A-PCL precursor. The change in the chemical shifts of the NH resonance indicates the formation of hydrogen-bonding interaction between adenine and uracil attached to chain ends of the A-PCL-U. Molecular weights and molecular weight distributions of PCL and A-PCL-U are listed in Table 1. In addition, number-average molecular weights are also calculated from the ^{1}H NMR integration ratios of the methylene signal on the PCL polymer backbone ($-OC{=}OCH_2-$, 3.9−4.2 ppm) to signal on the primary amine end group (NH_2-, 6.0 ppm).

Reversibility of Supermolecular Polymer. The reversibility of supramolecular polymer formation was investigated by using variable-temperature ^{1}H NMR spectroscopy in 1,1,2,2-tetrachloroethane-d_2 because the ability to form or break the hydrogen bonding by external stimuli is a key reason for the interest in these materials. The temperature dependence of the NH proton chemical shift of the A-PCL-U 4K complex at 10 wt % in 1,1,2,2-tetrachloroethane-d_2 is shown in Figure 2. The NH resonance shifts to upfield region systematically from 10.0 to 8.6 ppm as the temperature is raised from 25 to 100 °C. The gradual decrease in the

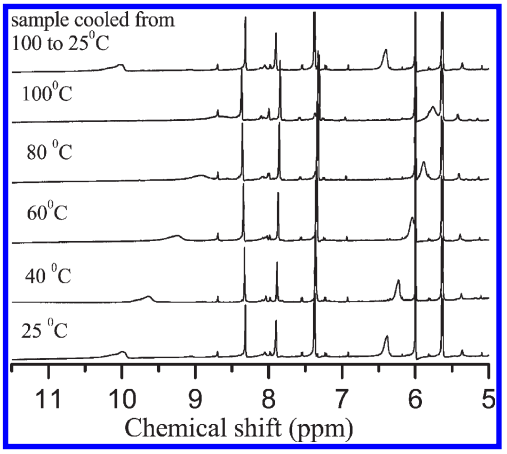

Figure 2. ^{1}H NMR NH chemical shift of the A-PCL-U 4K as a function of temperature (10 wt %). Sample was allowed to equilibrate for 10 min at each temperature.

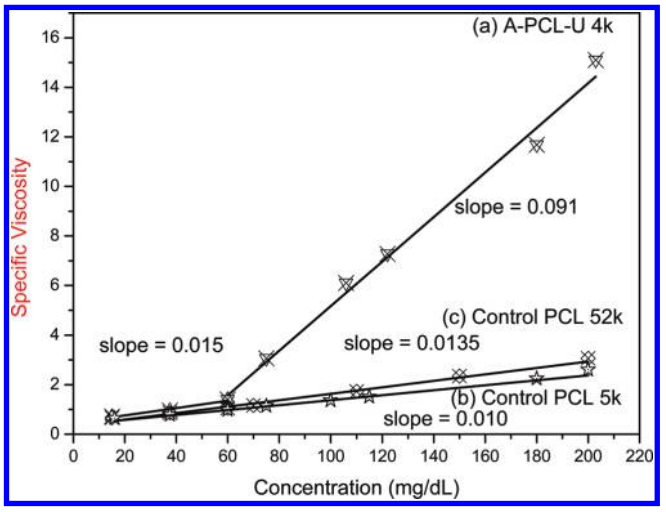

Figure 3. Plots of specific viscosity of A-PCL-U and control PCL in toluene solution vs concentration.

intensity of the NH resonance with increasing temperature can be attributed to the gradual dissociation of complementary hydrogen bonds.[44] However, as soon as the sample is cooled from 100 to 25 °C, the NH resonance returns to its original position at 10.0 ppm, suggesting that the nucleobase end-functionalized hydrogen-bonded supramolecular complexes are thermoreversible in 1,1,2,2-tetrachloroethane-d_2.

Solution Viscosity. The effect of hydrogen-bonding associations on solution viscosity of A-PCL-U in toluene at ambient temperature was measured using an Ubbelohde viscometer. Plots of specific viscosities (η_{sp}) of control PCL 5K and PCL 52K with respect to concentration ranging from 20 to 200 mg/dL are linear, indicating that there are no significant physical entanglements or noncovalent interactions between these control polymers. However, the formation of hydrogen-bonding interaction between adenine and uracil of A-PCL-U results in substantial increase in η_{sp} relative to that the PCL as shown in Figure 3. The connection of heteronucleobase units in solution driven by hydrogen-bonding interaction leads to an entangled reversible supramolecular heteropolymerization. The substantial increase in the solution viscosity of A-PCL-U relative to control PCL can be attributed to the formation of the supramolecular polymerization of A-PCL-U in solution.

^{1}H NMR Titration. Quantitative analysis for binding affinity of intermolecular heterocomplexation was obtained

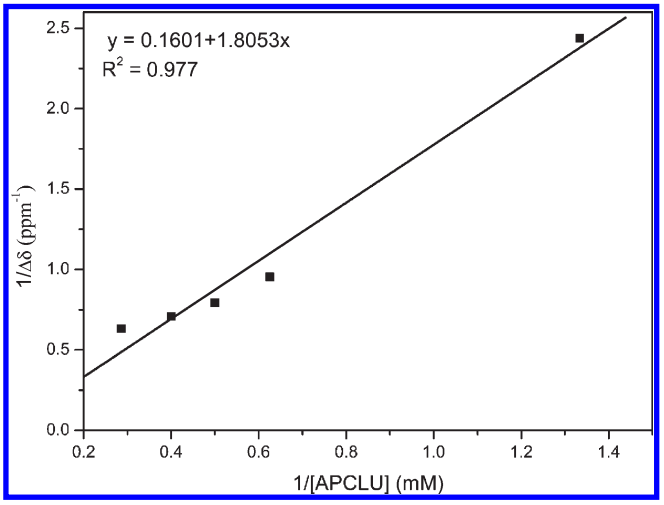

Figure 4. Benesi−Hildebrand plots adenine/uracil association in $CDCl_3$ (M_n = 4023, 27 °C).

via ^{1}H NMR titration experiment. The association constants (K_a) for hydrogen-bonded complexes characterized by 500 MHz ^{1}H NMR at 25 °C in chloroform-*d* and the A-PCL-U concentration systematically increased from 0.83 to 13.3 wt %. The position of the uracil N−H resonance in A-PCL-U shifts with increasing the concentration of the adenine. In addition, the resonances of the amido NHs are relatively broader, indicating a fast exchange rate between associated and dissociated A−U complex on the NMR time scale.[45] The Benesi−Hildebrand model, a mathematical method of determining the association constant (K_a) from NMR titration experiment, is employed to fit nonlinear chemical shift data for a dimeric hydrogen bond association with the assumption that the complex is formed in 1:1 stoichiometry using the following equation:[46,47]

$$\frac{1}{\Delta\delta} = \frac{1}{K_a \Delta\delta_{max}[\mathrm{APCLU}]} + \frac{1}{\delta_{max}} \qquad (1)$$

where $\Delta\delta_{max}$ is the maximum change of the chemical shift of the uracil NH protons. The slope of the double-reciprocal plot is $1/K_a\Delta\delta_{max}$, and the intercept is $1/\Delta\delta_{max}$. A double-reciprocal plot based on the association of A−U complex possesses a linear relationship as shown in Figure 4. The K_a obtained from the slope of the plot is 18.9 M^{-1}, which is consistent with K_a values reported previously for adenine−thymine (or adenine−uracil) base pair recognition (ca. 10−100 M^{-1} in $CDCl_3$).[25,48]

FTIR Analyses. After discovering the complementary behavior of A-PCL-U in solution, the assembly behavior of these complexes in the bulk state was investigated using FTIR spectroscopy at various temperatures (from 25 to 160 °C). Figure 5a illustrates FTIR spectra in the N−H stretching region of the A-PCL-U where the band at 3500 cm^{-1} corresponds to free amide NH group and peaks at 3320 and 3206 cm^{-1} are attributed to the A-U interaction. At 25 °C, the N−H stretching region (Figure 5a) shows a number of broad absorption bands in the 3200−3400 cm^{-1} region. Vibrations at 3206 and 3320 cm^{-1} correspond to medium strength hydrogen-bonded N-Hs,[37] implying that A-PCL-U indeed forms hydrogen-bonded interaction in the solid state. Upon heating from 25 to 160 °C, the signals at 3320 and 3206 cm^{-1}, corresponding to N−H stretching, shift toward higher wavenumber, and the free amide N−H stretching vibration at 3500 cm^{-1} increases gradually, indicating the change in the nature of the hydrogen bonding at high

temperature. In the 1640−1800 cm^{-1} region at 40 °C (Figure 5b), two carbonyl stretching peaks at 1734 and 1724 cm^{-1} correspond to the amorphous and crystalline carbonyl stretching, respectively. Upon heating from 40 to 60 °C, the amorphous C═O band at 1734 cm^{-1} appears as the weakly hydrogen-bonded amide indicated by the existence of bands at 3320 and 3206 cm^{-1} (Figure 5a), implying that the melting of A-PCL-U starts around 60 °C where the hydrogen-bonded amide appears. Therefore, we can conclude that the crystallization effect is more sensitive to temperature than the hydrogen-bonding interaction within A-PCL-U.

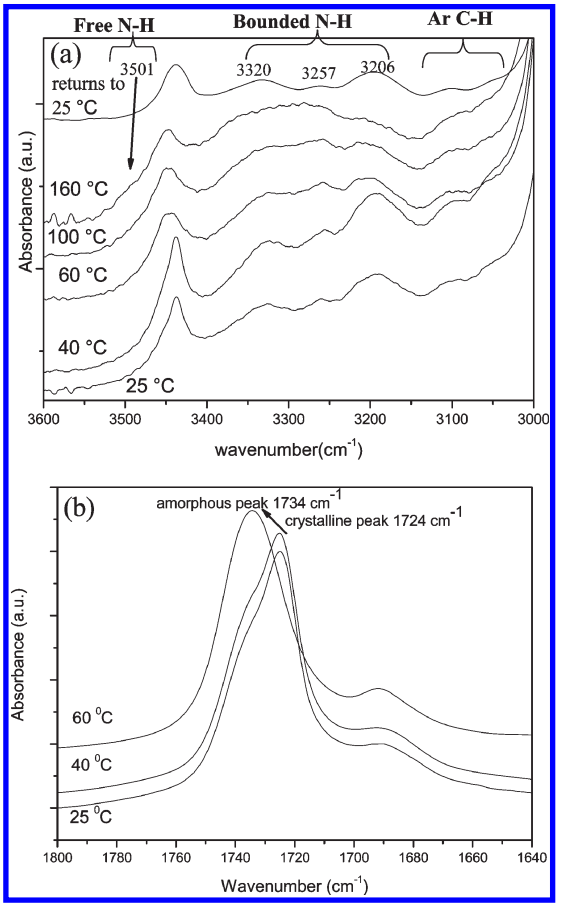

Figure 5. Variable temperature FT-IR spectra in the (a) 3000−3600 cm^{-1} region and (b) 1640−1800 cm^{-1} region of A-PCL-U 4K.

X-ray Diffraction Measurements. The wide-angle X-ray diffraction (WXRD) patterns between 3° and 40° reflecting the crystalline structure of the A-PCL-U sample are illustrated in Figure 6A. The diffraction peaks of the control PCL 5K agree well with those reported previously.[49] The intense diffraction peaks located at $2\theta = 21.39°$, 22.00°, and 23.70° are assigned to the (110), (111), and (200) reflections of PCL.[50] However, the diffraction peaks of the A-PCL-U shift to lower values of 2θ, implying that the crystalline structure of the A-PCL-U is different. During crystallization, the chain ends cannot be rejected from the early stage of the crystal growth and thus alter the final structure of PCL crystals.[51] To further investigate the effect of nucleobase on the A-PCL-U, the quenching treatment was carried out. These samples need to be quickly cooled down below −70 °C in order to avoid or reduce the crystallization of A-PCL-U from the disordered melt state. At −70 °C, a reflection at lower angle corresponding to *d*-spacing larger than 30 Å appears, implying that a significant reduction in the fraction of crystallization occurrs at the temperature.[30] However, careful comparison does show that both (110) and (200) peaks are reduced in intensity, and new diffraction peaks are apparently present. The new diffraction peak can be related to the hard segment because of the immisciblility between PCL and the terminal nucleobase hard segment units tends to self-assembled into microdomains. This observation does suggest that the crystal structure of the nucleobase-terminated PCL did change to a certain extent. Furthermore, the reflection peak at $2\theta = 19.4°$ ($d = 0.44$ nm) suggests that within these "hard" domains there are stacks of the nucleobase formed through $\pi-\pi$ interactions. Figure 6B illustrates the presence of a broader primary peaks and higher-order reflections at q/q^* ratios of 2 and 3 of A-PCL-U 5K, indicating that A-PCL-U is arranged as lamellae. The first peak located at the position of $q = 0.051$ nm^{-1} indicates the presence of a lamellar structure due to the occurrence of the long period 12.3 nm for A-PCL-U, which is also in good agreement with wide-angle X-ray diffraction analyses.

Thermal Analyses. For A-PCL-U and control PCL, DSC experiments were heated to 160 °C to fuse the crystals and then quenched to −90 °C for the second DSC scans. The second heating DSC thermograms of all A-PCL-U and PCL are shown in Figure 7. Essentially all A-PCL-U complexes

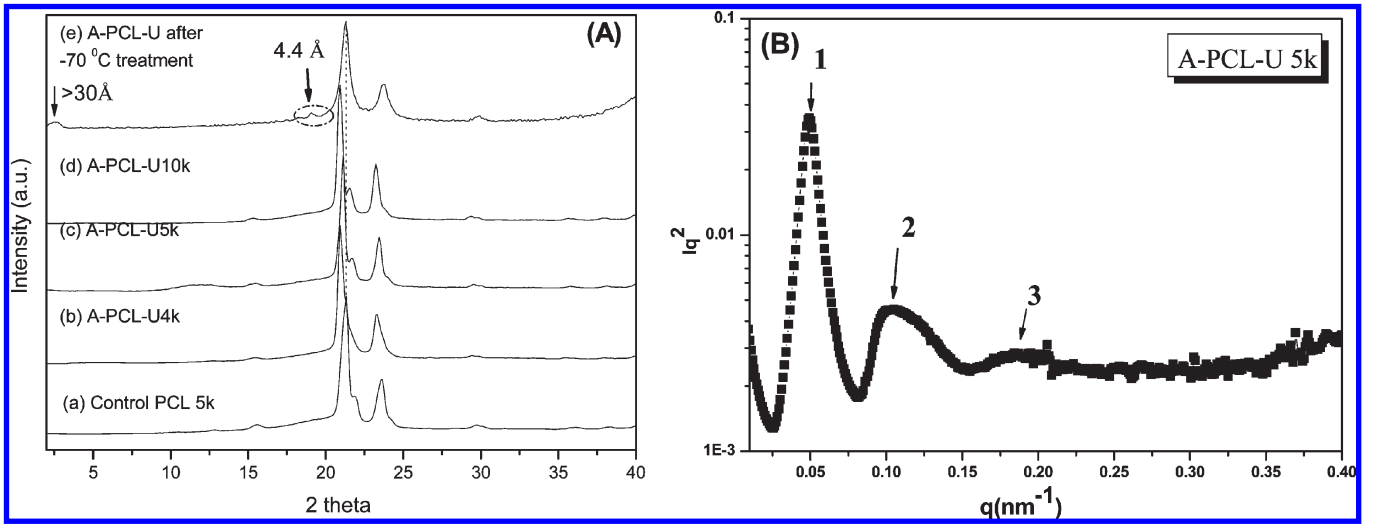

Figure 6. (A) XRD curves: (a) control PCL 5K, (b) A-PCL-U 4K, (c) A-PCL-U 5K, (d) A-PCL-U 10K, and (e) sample (a) after −70 °C. (B) Small-angle X-ray diffraction of A-PCL-U 5K recorded with Cu Kα X-ray radiation.

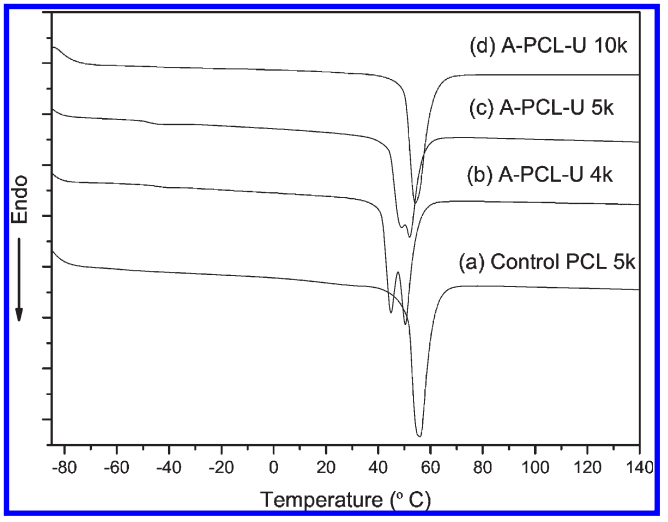

Figure 7. Heating DSC thermograms of pure and nucleobase-terminated PCL with variable molecular weights (second scans): (a) control PCL 5K, (b) A-PCL-U 4K, (c) A-PCL-U 5K, (d) A-PCL-U 10K.

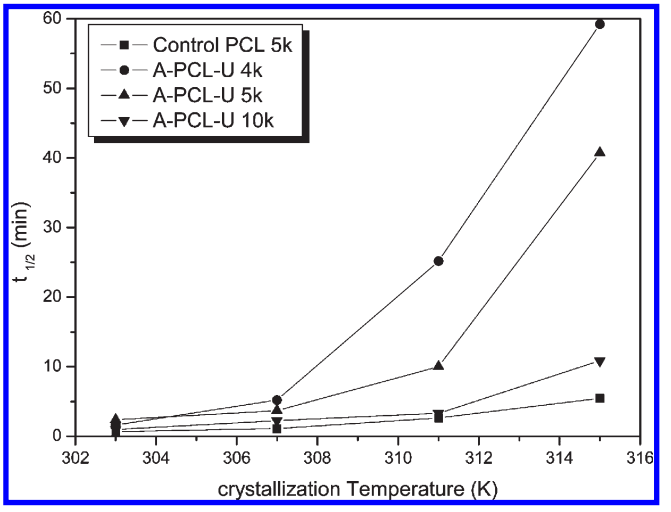

Figure 8. Plot of $t_{1/2}$ vs crystallization temperature for samples of control PCL and different molecular weight of nucleobase-terminated PCL.

display melting transitions at about 50 °C, which are lower than the control PCL. In addition, the melting temperature decreases with increasing the fraction of nucleobase unit in the complex, and the dual melting transitions are observed for those higher fraction nucleobase A-PCL-U as shown in Figure 7. The dual melting transitions of A-PCL-U can be attributed to melting of the initial crystals followed by recrystallization and final melting of the crystals grown during the heating scan.[52] To further investigate the thermal behaviors of A-PCL-U, DSC measurements were carried out (see the Supporting Information). All samples were first heated up to 80 °C at various heating rates and cooled at a rate of 10 °C/min. If the process is followed, when the heating rate is increased, the lower melting peak will be magnified, and the peak with higher melting temperature will decrease as shown in Figure S1. The higher melting peak was decreased with increasing heating rate. Therefore, the dual melting behavior is indeed originated from the recrystallization during the heating process. Since the A-PCL-U 10K does not show dual melting transition behavior, rearrangement through melting and recrystallization are retarded or even inhibited with low fraction of nucleobase units in the polymer chain. As a result, the content of the supermolecular binding motif in the bulk plays a critical role in affecting the crystallization behavior because of the phase segregation between the nucleobase pairs and polycaprolactone chains.

Isothermal Crystallization Kinetics. In order to study the isothermal crystallization kinetics, the weight fraction of crystallinity, $X(t)$, was calculated according to the follow equation:[53,54]

$$X(t) = \frac{\int_0^t \frac{dH}{dt}\,dt}{\int_0^\infty \frac{dH}{dt}\,dt} \qquad (2)$$

where the integral in the numerator is the heat generated at time t and that in the demominator is the total heat generated up to the end of the crystallization process. The typical isotherms data (see the Supporting Information) of these A-PCL-U and control PCL shows increasing in the end-functional concentration results in significant shift of the characteristic curves along the time axis, suggesting that the crystallization rate becomes progressively decreased.

Table 2. Values of n, k, and $t_{1/2}$ at Various T_c

	T_c (K)	n	k	$t_{1/2}$ (min)
control PCL 5K	303	2.7	6.7	0.67
	307	3.2	3.37	1.1
	311	2.8	0.56	2.65
	315	2.6	0.096	5.44
A-PCL-U 4K	303	2.7	0.41	1.605
	307	2.6	0.023	5.18
	311	2.8	0.00084	25.16
	315	2.7	0.00025	59.225
A-PCL-U 5K	303	2.7	0.41	2.365
	307	2.6	0.021	3.67
	311	2.8	0.00013	10.01
	315	2.8	0.0002	40.73
A-PCL-U 10K	303	2.8	3.48	0.945
	307	2.8	0.79	2.235
	311	2.8	0.077	3.31
	315	2.8	0.001	10.86

The crystallization kinetics is analyzed using the Avrami treatment:[55]

$$\log[-\ln(1-X(t))] = \log k + n \log(t) \qquad (3)$$

where $X(t)$ is the weight fraction of material crystallized after time t, n is the Avrami value which depends on both the nature of the primary nucleation and the growth geometry of the crystalline entities, and k is the overall kinetic rate constant which depends on rates of nucleation and growth. The values of k and n can be calculated from the intercept and slope of eq 3. The half-time of crystallization, $t_{1/2}$, is defined as the time required for half of the final crystallinity to be developed. The plots of $t_{1/2}$ as functions of T_c for various samples are shown in Figure 8, and the values of k, n, and $t_{1/2}$ are summarized in Table 2. The obtained noninteger n values in all cases are from mixed growth or surface nucleation modes. The value of k decreases with increasing the nucleobase concentration and the crystallization temperature. Results from the overall crystallization rate decrease with increasing the concentration of the nucleobase chain ends.[56]

Surface Morphology. Supramolecular binding motifs show well-defined fiberlike morphology due to the microphase separation of the hard block segments (such as adenine and uracil nucleobase pairs).[29,57] Similar structure is also expected to be present in the supramolecular polymers;[58] the microphase

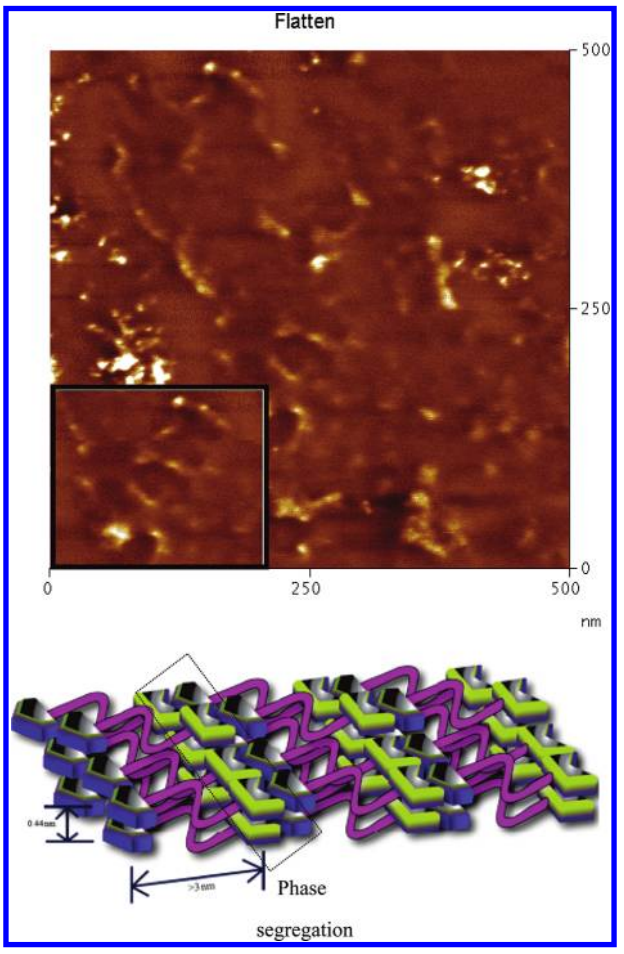

Figure 9. (a) AFM phase images at 500 nm scan sizes of A-PCL-U. *Z* ranges are 10 nm; $\Delta\varphi$ is 15° and 10°. Data obtained in tapping mode in air at 37 °C. In the phase images the hard phase of the polymer appears brighter than the soft phase. (b) Idealized phase-segregated morphology in the solid state.

separation between the hard and soft block domains was investigated with atomic force micoscopy (AFM) in the tapping mode regime. The thin polymer film dissoved in chloroform and then cast on a glass substrate. After evaporation of the solvent, the film is dried under vacuum at 40 °C. The phase image of A-PCL-U possesses a wormlike morphology where the bright parts are attributed to stack of hard segments of the complex as shown in Figure 9. In addition, the A-PCL-U shows disorder wormlike structure extending for several hundreds of nanometers from stacks of hard chain ends embedded in a soft matrix (Figure 9a). The wormlike dimension of the A-PCL-U domain is ~9 nm in diameter, and the spacing between these hard segments is in good agreement with the presence of a low angle peak (2θ = 2.5°) in the WXRD pattern. A small-angle diffraction pattern was also been observed in A-PCL-U although the peak was broad and relatively weak (Figure 6B). The profile for A-PCL-U has integer number of ordered peaks which reflects lamellar structure. Considering these experiments and AFM data, we can depict lamellar organization in which the molecules should be arranged into layer plane (Figure 9b). Furthermore, the molecules should form linear polymolecular chains through multiple complementary hydrogen bonds. It is likely that the wormlike hard domain consists of chain end stacks via hydrogen bonding between these hard chain ends (Figure 9b). In summary, the phase segregation between the aggregated hard nucleobase chain ends through aromatic amide hydrogen bonding and the soft polycaprolactone chains results in wormlike hard domains.

Summary

Ring-opening polymerization and Micheal addition reaction were employed to synthesize heteronucleobase (A and U)-functionalized PCL. Incorporation of multiple hydrogen-bonding units into PCL chain ends results in phase separation and dramatical increased viscosity as a result of the formation of supramolecular complexes chain. The K_a value of the A-PCL-U 4K is calculated as 18.9 M^{-1} using NMR measurements. In the bulk state, FTIR spectroscopies provide positive evidence for hydrogen-bonding interactions within these hard nucleobase chain ends. In addition, WXRD and DSC measurements further provide evidence that the crystalline structure of the A-PCL-U is changed to some extent due to phase segregation between the hard chain ends and the polycaprolactone chains. The SAXS technique has been employed to investigate in detail the presence of a broader primary peaks and higher-order reflection at q/q^* ratios of 2 and 3 of A-PCL-U 5K, indicating that A-PCL-U is arranged as lamellae. Furthermore, AFM surface morphology shows phase separation of end-group aggregation through hydrogen-bonding interaction in the form of wormlike structure.

Acknowledgment. This study was supported financially by the National Science Council, Taiwan (Contract NSC-98-2221-E-009-006).

Supporting Information Available: Results about DSC of A-PCL-U analyses. This material is available free of charge via the Internet at http://pubs.acs.org.

References and Notes

(1) Saenger, W. *Principles of Nucleic Acid Structures*; Springer: Berlin, 1984.
(2) Soyfer, V. N.; Potaman, V. N. *Triple-Helical Nucleic Acids*; Springer: New York, 1995.
(3) Binder, W. H.; Zirbs, R. *Adv. Polym. Sci.* **2007**, *207*, 1.
(4) Bernard, J.; Lortie, F.; Fenet, B. *Macromol. Rapid Commun.* **2009**, *30*, 83.
(5) Sirringhaus, H.; Kawase, T.; Friend, R. H.; Shimoda, T.; Inbasekaran, M.; Wu, W.; Woo, E. P. *Science* **2000**, *290*, 2123.
(6) Ziauddin, J.; Sabatini, D. M. *Nature* **2001**, *411*, 107.
(7) Whitesides, G. M.; Ostuni, E.; Takayama, S.; Jiang, X. Y.; Ingber, D. E. *Annu. Rev. Biomed. Eng.* **2001**, *3*, 335.
(8) Kataoka, D. E.; Troian, S. M. *Nature* **1999**, *402*, 794.
(9) Delamarche, E.; Bernard, A.; Schmid, H.; Bietsch, A.; Michel, B.; Biebuyck, H. *J. Am. Chem. Soc.* **1998**, *120*, 500.
(10) Feldman, K. E.; Kade, M. J.; Meijer, E. W.; Hawker, C. J.; Kramer, E. J. *Macromolecules* **2009**, *42*, 9072.
(11) Khan, A.; Haddleton, D. M.; Hannon, M. J.; Kukulj, D.; Marsh, A. *Macromolecules* **1999**, *32*, 6560.
(12) Nair, K. P.; Breedveld, V.; Weck, M. *Macromolecules* **2008**, *41*, 3429.
(13) Xu, J.; Fogleman, E. A.; Craig, S. L. *Macromolecules* **2004**, *37*, 1863.
(14) Boal, A. K.; Ilhan, F.; DeRouchey, J. E.; Thurn-Albrecht, T.; Russell, T. P.; Rotello, V. M. *Nature* **2000**, *404*, 746.
(15) Lutz, J. F.; Thuenemann, A. F.; Rurack, K. *Macromolecules* **2005**, *38*, 8124.
(16) Schmatloch, S.; van den Berg, A. M. J.; Alexeev, A. S.; Hofmeier, H.; Schubert, U. S. *Macromolecules* **2003**, *36*, 9943.
(17) Saito, N.; Murakami, N.; Takahashi, J.; Horiuchi, H.; Ota, H.; Kato, H.; Okada, T.; Nozaki, K.; Takaoka, K. *Adv. Drug Delivery Rev.* **2005**, *57*, 1037.
(18) Kim, S. S.; Park, M. S.; Jeon, O.; Choi, C. Y.; Kim, B. S. *Biomaterials* **2006**, *27*, 1399.
(19) Zou, S.; Schroenherr, H.; Vancso, G. J. *Angew. Chem., Int. Ed.* **2005**, *44*, 956.
(20) Roland, J. T.; Guan, Z. *J. Am. Chem. Soc.* **2004**, *126*, 14328.
(21) Guan, Z.; Roland, J. T.; Bai, J. Z.; Ma, S. X.; McIntire, T. M.; Nguyen, M. *J. Am. Chem. Soc.* **2004**, *126*, 2058.

(22) Spijker, H. J.; Dirks, A. J.; Van Hest, J. C. M. *J. Polym. Sci., Part A: Polym. Chem.* **2006**, *44*, 4242.
(23) Muthukumar, M.; Ober, C. K.; Thomas, E. L. *Science* **1997**, *277*, 1225.
(24) Rieth, S.; Baddeley, C.; Badjic, J. D. *Soft Matter* **2007**, *3*, 137.
(25) Sivakova, S.; Rowan, S. J. *Chem. Soc. Rev.* **2005**, *34*, 9.
(26) Yamauchi, K.; Lizotte, J. R.; Long, T. E. *Macromolecules* **2002**, *35*, 8745.
(27) Snip, E.; Shinkai, S.; Reinhoudt, D. N. *Tetrahedron Lett.* **2001**, *42*, 2153.
(28) Dankers, P. Y. W.; Harmsen, M. C.; Brouwer, L. A.; Van Luyn, M. J. A.; Meijer, E. W. *Nat. Mater.* **2005**, *4*, 568.
(29) Rowan, S. J.; Suwanmala, P.; Sivakova, S. *J. Polym. Sci., Part A: Polym. Chem.* **2003**, *41*, 3589.
(30) Sivakova, S.; Bohnsack, D. A.; Mackay, M. E.; Suwanmala, P.; Rowan, S. J. *J. Am. Chem. Soc.* **2005**, *127*, 18202.
(31) Mather, B. D.; Baker, M. B.; Beyer, F. L.; Berg, M. A. G.; Green, M. D.; Long, T. E. *Macromolecules* **2007**, *40*, 6834.
(32) Shenhar, R.; Xu, H.; Frankamp, B. L.; Mates, T. E.; Sanyal, A.; Uzun, O.; Rotello, V. M. *J. Am. Chem. Soc.* **2005**, *127*, 16318.
(33) Binder, W. H.; Kluger, C.; Straif, C. J.; Friedbacher, G. *Macromolecules* **2005**, *38*, 9405.
(34) Thibault, R. J.; Hotchkiss, P. J.; Gray, M.; Rotello, V. M. *J. Am. Chem. Soc.* **2003**, *125*, 11249.
(35) Mueller, A.; Talbot, F.; Leutwyler, S. *J. Am. Chem. Soc.* **2002**, *124*, 14486.
(36) Viswanathan, K.; Long, T. E.; Ward, T. C. *J. Polym. Sci., Part A: Polym. Chem.* **2005**, *43*, 3655.
(37) Shimizu, T.; Iwaura, R.; Masuda, M.; Hanada, T.; Yase, K. *J. Am. Chem. Soc.* **2001**, *123*, 5947.
(38) Iwaura, R.; Yoshida, K.; Masuda, M.; Ohnishi-Kameyama, M.; Yoshida, M.; Shimizu, T. *Angew. Chem., Int. Ed.* **2003**, *42*, 1009.
(39) Iwaura, R.; Yoshida, K.; Masuda, M.; Yase, K.; Shimizu, T. *Chem. Mater.* **2002**, *14*, 3047.
(40) Cheng, C. C.; Huang, C. F.; Yen, Y. C.; Chang, F. C. *J. Polym. Sci., Part A: Polym. Chem.* **2008**, *46*, 6416.
(41) Cheng, C. C.; Yen, Y. C.; Ye, Y. S.; Chang, F. C. *J. Polym. Sci., Part A: Polym. Chem.* **2009**, *47*, 6388.
(42) Kuo, S. W.; Huang, C. F.; Lu, C. H.; Chang, F. C. *Macromol. Chem. Phys.* **2006**, *207*, 2006.
(43) Ustyuzhanin, G. E.; Kolomeitseva, V. V.; Tikhomirova-Sidorova, N. S. *Khim. Geterotsikl. Soedin.* **1978**, *5*, 684.
(44) Karikari, A. S.; Mather, B. D.; Long, T. E. *Biomacromolecules* **2007**, *8*, 302.
(45) Park, T.; Zimmerman, S. C. *J. Am. Chem. Soc.* **2006**, *128*, 11582.
(46) Fielding, L. *Tetrahedron* **2000**, *56*, 6151.
(47) Mesplet, N.; Morin, P.; Ribet, J. P. *Eur. J. Pharm. Biopharm.* **2005**, *59*, 523.
(48) Kyogoku, Y.; Lord, R. C.; Rich, A. *Biochim. Biophys. Acta* **1969**, *179*, 10.
(49) Hu, H.; Dorset, D. L. *Macromolecules* **1990**, *23*, 4604.
(50) Nojima, S.; Hashizume, K.; Rohadi, A.; Sasaki, S. *Polymer* **1997**, *38*, 2711.
(51) Ni, Y.; Zheng, S. *J. Polym. Sci., Part B: Polym. Phys.* **2007**, *45*, 2201.
(52) Wunderlich, B. *Macromolecular Physics*; Academic: London, 1973; Vols. *1*−*3*.
(53) Mancarella, C.; Martucelli, E. *Polymer* **1977**, *13*, 407.
(54) Wunderlich, B. *Macromolecular Physics*; Academic Press: New York, 1976.
(55) Avrami, M. *J. Chem. Phys.* **1939**, *7*, 1103.
(56) Kuo, S. W.; Chan, S. C.; Chang, F. C. *J. Polym. Sci., Part B: Polym. Phys.* **2004**, *42*, 117.
(57) Dankers, P. Y. W.; Zhang, Z.; Wisse, E.; Grijpma, D. W.; Sijbesma, R. P.; Feijen, J.; Meijer, E. W. *Macromolecules* **2006**, *39*, 8763.
(58) Wisse, E.; Spiering, A. J. H.; van Leeuwen, E. N. M.; Renken, R. A. E.; Dankers, P. Y. W.; Brouwer, L. A.; van Luyn, M. J. A.; Harmsen, M. C.; Sommerdijk, N. A. J. M.; Meijer, E. W. *Biomacromolecules* **2006**, *7*, 3385.